Dispersion and anisotropy of the optical second-harmonic response of single-crystal Al surfaces

S. Janz, K. Pedersen,* and H. M. van Driel
Department of Physics, University of Toronto, Toronto, Ontario, Canada M5S-1A7
(Received 23 January 1991; revised manuscript received 16 April 1991)

We have performed tests of recent theories for the surface second-harmonic (SH) response of a jellium metal by measuring the dispersion characteristics of SH generation from atomically clean Al(111), Al(110), and Al(100) surfaces. This has been done for wavelengths between 565 and 860 nm, by using a picosecond-pulse dye-laser beam incident at angles of 22.5°, 45°, and 67.5°. In all cases, only *p*-polarized SH light generated by *p*-polarized incident light was observed. Absolute magnitudes were obtained by normalizing the SH response to that of a quartz plate. Contrary to expectations for a jellium metal, the Al(110) and Al(111) faces each yielded an anisotropic SH response, the intensity varying as the specimens were rotated about their surface normals. The relative magnitude of the anisotropic component increased with increasing wavelength and decreasing angle of incidence. By studying the variation of the SH intensity with temperature and oxygen exposure, we conclude that the anisotropic component is not due to intrinsic electronic effects but rather to the always-present atomic steps on the surface. We thereafter show that the isotropic component of the SH response can be identified with the flat ideally terminated surface. For all three surfaces, the characteristics of the isotropic SH response, in terms of magnitude and wavelength dependence, agree best with the recent results of calculations by Liebsch and Schaich [Phys. Rev. B **40**, 5401 (1989)] employing the local-density approximation to calculate the ground-state electron distribution and the random-phase approximation to evaluate the SH response. The only significant deviation from this agreement is observed for Al(100) near 820 nm where an increasing SH response with increasing wavelength is attributed to a surface-state resonance.

I. INTRODUCTION

Second-harmonic (SH) generation from centrosymmetric solids and liquids has attracted considerable attention as an optical probe of surfaces of centrosymmetric materials.[1] This surface sensitivity arises because the breaking of inversion symmetry at the surface allows for a dipolar SH response, whereas this is not permitted in the bulk. In particular, SH generation from metal and semiconductor surfaces has proven to be of fundamental and applied interest for 25 years since the first experiments of Brown *et al.* on Ag surfaces.[2,3] However, the interpretation of early results was hampered by the effects of adsorbed oxygen and other contaminants for samples maintained in air or moderate vacuum. More recently, the recognition of having to work with well-characterized samples in ultrahigh vacuum (UHV) has led to significant advances in our understanding of the nonlinear optical response of surfaces.[4–6] At the same time surface SH generation has proven to be a powerful probe of adsorption of gases at surfaces,[7,8] surface structure,[9] and surface chemical processes.[10,11]

For semiconductor surfaces, the understanding of both the magnitude and dispersion of the SH response remains at a phenomenological level.[12,13] On the other hand, microscopic theories for the origin of SH generation from metal surfaces have been put forward for more than 20 years,[14–16] and recently calculations have advanced to the point where comparisons between theory and experiment are meaningful. Early models[14,15] were based upon step-function surface electron distributions, and used the jellium approximation in which the effects of the lattice potential are ignored. Although more recent, sophisticated calculations[16,17] still employ the jellium approximation, they employ more realistic surface potentials and electron-density profiles, and are based on a self-consistent, many-body quantum-mechanical response theory. Such models make the evaluation of the nonlinear optical response in the surface region tractable and provide reasonable approximations to nearly-free-electron metals such as Al and (for infrared incident light) Ag. On the basis of these models, SH generation now provides one of the most rigorous tests of our understanding of the linear and nonlinear electromagnetic response of metals.

In this paper we present the results of a systematic experimental investigation of the dispersion characteristics of SH generation from Al. These measurements have been performed for Al(111), Al(110), and Al(100) surfaces over the wavelength range $560 < \lambda < 860$ nm with picosecond laser pulses that induce minimal heating effects. These measurements provide the first significant test of the dispersion characteristics predicted by theoretical models. We have also performed experiments to explore the influence of the lattice potential and surface morphology in determining the anisotropy of the SH response (i.e., a dependence of the SH efficiency on the relative orientation of the incident field and the crystal axes).

In previous work, it has been demonstrated by Murphy *et al.*[5] that the SH response of an Al(111) surface at an incident wavelength of 1.06 μm agrees very closely with the self-consistent density-functional calculations of Liebsch and Schaich.[16] On the other hand, the same workers observed an anisotropy in the SH response of the

Al surface both with respect to the azimuthal rotation of the crystal about the surface normal and with respect to the response of the different crystal faces. These results indicate that the SH response of Al may not be entirely free electron like. Results for Cu (Ref. 4) and Ni (Ref. 8) also demonstrate that the SH response of a metal surface will in general have an anisotropic component. However, recent experimental results for stepped Si(Ref. 18) and Al (Ref. 19) surfaces indicate that the presence of steps on a surface can induce a significant anisotropy which is not due to intrinsic electronic structure. In previous work in this laboratory, it has been shown that the anisotropic response of surface steps on Al can be identified from the anomalous variation of the SH signal with oxygen exposure[19] and temperature.[20] We have therefore studied the dependence of the SH signal on oxygen exposure and temperature to identify the source of the observed anisotropy.

The rest of this paper is organized as follows. In Sec. II we outline the theory of SH response from centrosymmetric materials, and metals in particular. We present the salient features necessary for us to interpret our results. Section III contains the details of the experimental techniques and describes the experiments which have been performed to measure the wavelength dependence and the anisotropy of the SH signal, as well as the variation of the SH response with temperature and oxygen exposure. In Sec. IV we offer experimental results and compare, where appropriate, results with theoretical calculations. Conclusions from the work are described in Sec. V.

II. THEORY

The general phenomenological theory for SH generation from cubic centrosymmetric materials has been developed by several different workers over the last decade.[13,21–23] The overall second-order polarization density can be written as the sum of bulk electric quadrupole and/or magnetic dipole terms and surface electric dipole terms. For an incident monochromatic plane wave the bulk polarization is given by

$$P_i^B(2\omega)=\gamma(\omega)\nabla_i(\mathbf{E}\cdot\mathbf{E})+\zeta(\omega)\mathrm{E}_\mathrm{i}\nabla_\mathrm{i}\mathrm{E}_\mathrm{i}\ , \tag{1}$$

where $\mathbf{E}$ is the field inside the metal, $\gamma(\omega)$ and $\zeta(\omega)$ are phenomenological parameters dependent on frequency, and the coordinate system is defined by the edges of the cubic unit cell. The first term gives rise to an isotropic polarization, whereas the second term will contribute to an anisotropic SH response of the metal. The surface SH polarization can be treated as a polarization sheet located just above the surface of the metal. The corresponding SH polarization density can be written in terms of the surface response tensor χ_{ijk} as

$$P_i^S(2\omega)=\chi_{ijk}(2\omega,\omega,\omega)E_jE_k\delta(z-z_0^+)\ , \tag{2}$$

where the surface is at $z=z_0$ and the incident field E is evaluated just inside the surface. The coordinate system is chosen such that the z axis is normal to the surface and the x axis is the projection of the [100] axis onto the surface.

While the theory for the SH response of centrosymmetric semiconductors has remained strictly phenomenological, for metals several authors have provided a microscopic model for the SH response on the basis of the isotropic jellium model. The SH response of a jellium metal consists of a surface polarization $\mathbf{P}^S(2\omega)$ parametrized by the Rudnick and Stern $a(\omega)$ and $b(\omega)$ coefficients,[14] and a bulk polarization $\mathbf{P}^B(2\omega)$ parametrized by a third coefficient $d(\omega)$.[15] These two terms are given by

$$\mathbf{P}^S(2\omega)\sim a(\omega)E_zE_zf\hat{\mathbf{z}}+b(\omega)E_zE_xg\hat{\mathbf{x}} \tag{3a}$$

and

$$\mathbf{P}^B(2\omega)\sim\gamma(\omega)d(\omega)\nabla(\mathbf{E}\cdot\mathbf{E})\ , \tag{3b}$$

where the constants f and g involve the linear properties of the metal. Here $a(\omega)$ determines the induced SH polarization oscillating normal to the surface (i.e., the $\hat{\mathbf{z}}$ direction), while $b(\omega)$ determines the SH polarization in a direction parallel to the surface (the $\hat{\mathbf{x}}$ direction). The bulk SH polarization, due to the magnetic dipole response, corresponds to the isotropic term involving $\gamma(\omega)$ in Eq. (1), where for a free-electron gas $\gamma(\omega)=e^3n/8m^2\omega^4$ and $d=1$,[15] with n, m, and $-e$ being the electron density, mass, and charge, respectively. On the other hand, the anisotropic parameter $\zeta(\omega)$ in Eq. (1) is obviously zero for a jellium metal. The surface susceptibility tensor χ_{ijk} in Eq. (2) can be expressed in terms of the Rudnick and Stern parameters as follows:

$$\chi_{zzz}=\frac{a(\omega)ne^3}{4m^2\omega^4}\ , \tag{4a}$$

$$\chi_{xzx}=\chi_{yzy}=\frac{b(\omega)ne^3}{2m^2\omega^4}\ . \tag{4b}$$

The objective of the jellium model calculations is to find $a(\omega)$ and $b(\omega)$ for a given metal surface. Such a calculation involves the evaluation of the ground state of the electron gas in the surface region, the evaluation of the screened linear fields, and finally the calculation of the SH polarization induced by the linear fields. Several authors[14,15] have shown that the parallel surface polarization coefficient $b(\omega)$ and the bulk polarization coefficient $d(\omega)$ are given by $b(\omega)=-1$ and $d(\omega)=1$, and are insensitive to incident frequency and the exact shape of the surface potential. Determining $a(\omega)$, on the other hand, requires a detailed calculation of the linear and SH response in the surface region. As discussed in detail in Ref. 16, the main feature that distinguishes different jellium model calculations is the treatment of the surface potential. Rudnick and Stern,[14] who carried out a semiclassical derivation for an infinite barrier surface potential and an electron density corresponding to Ag, obtained $a(0)=-1.06$. Calculations by Corvi and Schaich[15] for a finite step surface potential yielded $a(0)=-\frac{2}{9}$, independent of electron density. In contrast to these results for step potentials, the calculated $a(0)$ values obtained from models employing more realistic surface potentials and electron densities are an order of magnitude larger. These models are based on the density-functional theory for jellium surfaces developed by Lang and Kohn.[24] The

density-functional approach was first used by Weber and Liebsch[25] to evaluate the SH response of a metal surface in the low-frequency limit, resulting in a value of $a(0)=12.9$ for Ag. The density-functional approach was then extended to finite frequencies by Liebsch and Schaich.[16] In this approach, density-functional theory, in the local-density approximation (LDA), is used to calculate the ground state of the metal surface. The time-dependent LDA density-functional method (TDLDA) is then used to calculate the a coefficient of the surface. The main advantage of this technique is that a realistic ground-state electron-density profile and the corresponding surface potential are used as the starting point for the SH response calculation. Using this method, Liebsch and Schaich obtained $a(0)=28.4$ for an electron density appropriate for Ag. The close agreement with this result by Chizmeshya and Zaremba[17] [$a(0)=34.7$], who used a semiclassical extended Thomas-Fermi model, indicates that the most important element of these calculations is the correct treatment of the surface potential.

The TDLDA method also incorporates exchange-correlation effects into the evaluation of the SH response. This calculation predicts that a large part of the SH polarization is located in the electron-density tail outside the surface, and the authors have pointed out that including exchange-correlation effects may cause the net SH response to be overestimated because the LDA is not valid at low densities. Therefore the SH response of the LDA ground state was also derived using the random-phase approximation (LDA-RPA) to calculate $a(\omega)$, giving results that were approximately 25% smaller than the full LDA calculation in the optical and near-infrared frequency range.

One drawback of a jellium model for determining the SH response is that it neglects the influence of the lattice potential. The lattice potential modifies the shape of the surface potential, which will in general differ from the screened square-well potential derived using the jellium model.[24] Since the SH response is known to be sensitive to the shape of the surface potential,[16] the real surface may produce a SH response very different from that of a jellium surface. In addition, the interband contribution to the SH response will cause changes in the frequency dependence of the SH polarization.

The lattice potential may also introduce anisotropic contributions to the total SH response.[4,5] Thus the SH intensity can vary as the specimen is rotated about its surface normal, with the angular period of modulation depending on the symmetry of the crystal face. For example, using the formalism of Sipe, Moss, and Van Driel[13] the radiated p-polarized SH field from a (111) or a (110) surface irradiated by a p-polarized incident beam will have the general form

$$E(2\omega)=A'+B'\cos(M\psi)\ , \tag{5}$$

where $M=3$ for a (111) surface and $M=2$ for a (110) surface. The azimuthal angle ψ is the angle between the component of the incident-light wave vector parallel to the surface and the x axis. The coefficients A' and B' depend on the surface susceptibility tensor χ_{ijk}, the bulk response coefficients $\gamma(\omega)$ and $\zeta(\omega)$, and the fundamental linear optical parameters of the material. Note that because of the symmetry of the (100) surface, there is no surface contribution to the anisotropic coefficient B' for a (100) surface.

Clearly, a metal responding like an ideal jellium system will have only an isotropic response. Conversely, the presence of anisotropy in the SH response may indicate that the lattice potential, and hence the electronic band structure, is playing a significant role in determining the SH response. However, it may also be possible that the anisotropic response is due to features of the microscopic surface morphology, such as steps,[18,19] which will reflect the symmetry of the underlying lattice structure. In Sec. III we discuss in more detail how the temperature and oxygen exposure dependence of the anisotropic SH signal may be used to distinguish the contribution due to electronic band structure and that due to surface morphology.

The variation of the anisotropic SH response with incident wavelength can yield information on how band structure or surface morphology determines the SH polarization. On the other hand, since the free-electron contribution to the SH response is isotropic, a comparison of experimental measurements with jellium model results requires the extraction of the isotropic component of the SH signal from the data by inverting Eq. (5). To carry out this inversion one must measure the variation of the SH signal with azimuthal angle ψ. We conclude that in order to test theoretical calculations of the SH response of a metal surface it is necessary to make measurements of both the isotropic and the anisotropic parts of the SH signal.

To test the different theories the quantity one usually measures is the ratio R of the SH intensity $I_{2\omega}$ to the square of the incident intensity I_ω,

$$R\equiv I_{2\omega}/I_\omega^2\ . \tag{6}$$

For a jellium metal the value of R is determined by $a(\omega)$, $b(\omega)$, and $d(\omega)$, the dielectric constant $\epsilon(\omega)$, the angle of incidence θ, and the polarization angle ϕ (i.e., the angle between the incident electric-field vector and the plane of incidence). For p-polarized SH light R is given by[16]

$$R=\frac{8\pi e^2}{m^2\omega^2c^3}\left|\frac{\epsilon(\omega)[\epsilon(\omega)-1]}{\epsilon(2\omega)+s(2\omega)}(P\cos^2\phi+S\sin^2\phi)\tan\theta\right|^2\ , \tag{7}$$

where

$$P=\left[a(\omega)\frac{\epsilon(2\omega)}{\epsilon(\omega)}\sin^2\theta-b(\omega)\frac{2s(\omega)s(2\omega)}{\epsilon(\omega)}\cos^2\theta+d(\omega)/2\right]\Big/[\epsilon(\omega)+s(\omega)]^2\ ,$$

and

$$S=d(\omega)/2\epsilon(\omega)[1+s(\omega)]^2\ ,$$

and the function $s(\omega)$ is given by

$$s(\omega)=[\epsilon(\omega)-\sin^2\theta]^{1/2}/\cos\theta\ .$$

The corresponding expression for R in the case of s-polarized SH light gives a value much smaller than for the p-polarized case, as long as $|a(\omega)| \gg |b(\omega|$. If the SH response of the metal has anisotropic contributions as well, the radiated SH field will have the form of Eq. (5), and hence R will have the phenomenological form

$$R = |A + B\cos(M\psi)|^2 . \quad (8)$$

In this case, the jellium response given in Eq. (7) will only contribute to the isotropic coefficient A in Eq. (8).

In order to obtain absolute measurements of the SH reflectivity which can be compared with theory, it is necessary to normalize the SH intensity from the Al specimen relative to the signal from a reference material with a known SH susceptibility. In the experiment described here we use a single-crystal quartz plate for a reference source because its nonlinear optical properties are thoroughly understood,[26] and also because there are no strong interband transitions in the wavelength range of interest which could give rise to a strong wavelength dependence of the SH signal. Converting the normalized measurements of the SH response to absolute values requires a knowledge of the SH susceptibility of quartz over the entire wavelength range used in this study. However, the SH susceptibility $\chi^{(2)}_{111}$ of quartz has only been measured for an incident wavelength of 1.06 μm.[27] In the experiments described here, the incident and SH photon energies are always well below the quartz interband transitions at $\sim$7 eV. Therefore the dispersion in the SH susceptibility will be small, and it is a reasonable approximation to assume that $\chi^{(2)}_{111}$ is constant over the incident wavelength range. Alternatively, we can make use of Miller's rule[28] to obtain a better estimate of $\chi^{(2)}_{111}(2\omega)$ for quartz. Miller's rule states that the SH susceptibility of a material is proportional to a product of linear susceptibilities, $\chi^{(1)}_{ii}(\omega)$, as follows:

$$\chi^{(2)}_{ijk}(2\omega) = \chi^{(1)}_{ii}(2\omega)\chi^{(1)}_{jj}(\omega)\chi^{(1)}_{kk}(\omega)\Delta_{ijk} , \quad (9)$$

where Miller's coefficient Δ_{ijk} is a constant. It has been demonstrated experimentally[29,30] for several different materials that the dispersion of Δ_{ijk} is much smaller than the corresponding dispersion in the SH susceptibility $\chi^{(2)}(2\omega)$, even when the SH frequency is at strong interband resonances of a given material. The bond-charge model of Levine[31] predicts that for incident frequencies well below the interband transitions, the SH susceptibility of a material will satisfy Miller's rule. Furthermore, a calculation of $\chi^{(2)}_{111}(2\omega)$ for quartz at $\lambda = 1.06$ μm using the bond-charge model[31] agrees with experiment to within 2%. Therefore, since the bond-charge model gives a correct description of the SH response of quartz at 1.06 μm, we expect that Miller's rule will be a reasonable approximation over the wavelength range used in these experiments. Knowing that $\chi^{(2)}_{111}(2\omega) = 1.9\times10^{-2}$ esu at $\lambda = 1.06$ μm,[27] we use Miller's rule to estimate the SH susceptibility at the wavelengths used in these experiments. As expected, the estimated increase of $\chi^{(2)}_{111}(2\omega)$ with wavelength from 1.06 μm to 565 nm is only about 15%, indicating that the interband transitions in quartz do not have a significant effect in this wavelength range.

III. EXPERIMENT

A schematic diagram of the experimental setup used to determine the SH dispersion is shown in Fig. 1. The Al specimens were mounted in an ultra high vacuum (UHV) chamber capable of reaching pressure below 4×10^{-10} Torr. The UHV chamber has three quartz glass viewports so that SH experiments can be carried out at incident angles $\theta = 67.5°$, 45°, and 22.5°. The sample holder has two independent axes of rotation so that θ and the azimuthal angle ψ could be varied *in situ*, with ψ having the range $0° < \psi < 140°$. The chamber also has low-energy electron diffraction (LEED) and Auger-electron spectroscopy (AES) ports for structural and chemical surface characterization. The specimen temperature could be varied between -100 °C and 700 °C using a resistive heater and liquid-N_2 cooling. Temperatures were measured using a thermocouple in thermal contact with the specimen.

Each specimen was prepared from a single-crystal Al disk oriented using Laue x-ray diffraction and cut to within 1° of the desired crystallographic orientation. The specimen surface was mechanically polished to a mirror finish and mounted in a strain-free manner in the UHV chamber. The specimen was cleaned using cycles of 1-keV argon ion bombardment and annealing at 450 °C. These cycles were repeated until a sharp single-crystal LEED pattern was obtained from the surface and the contamination of the surface, mainly by carbon and oxygen, was determined by AES to correspond to less than 1% of a monolayer.

It has been demonstrated experimentally that rough metal surfaces, prepared either electrochemically[32,33] or

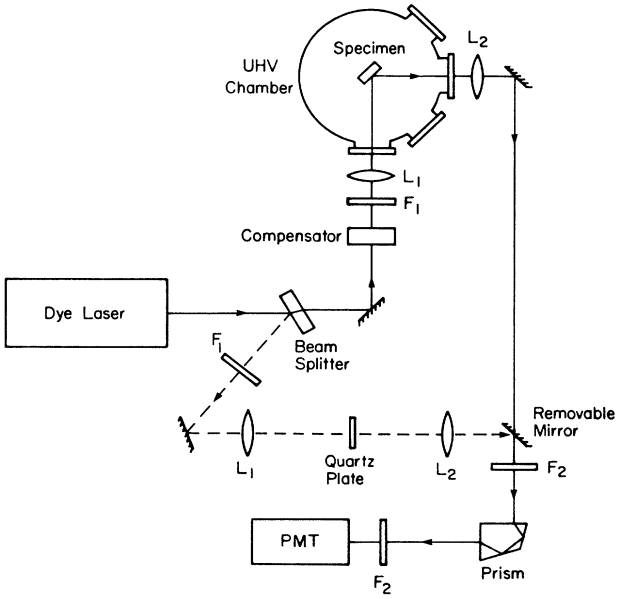

FIG. 1. The experimental arrangement for measuring the SH intensity generated at an Al surface in UHV relative to the SH intensity from a quartz plate. $L1$ and $L2$ are 25-cm focal-length lenses. The filters $F1$ block SH light and transmit the fundamental, while filters $F2$ block the fundamental and transmit the SH light.

by evaporating the metal onto a rough substrate,[34] exhibit an enhancement of the SH intensity of up to three orders of magnitude. The roughness reported in these experiments ranged from small superatomic roughness consisting of features typically 10-Å high and 20 Å in width,[33] to larger scale roughness with surface height modulations at length scales from several hundred to 1000 Å.[34] The large SH enhancements are attributed to local-field enhancement arising from a concentration of the incident-field intensity near the tips of surface protrusions (i.e., the lightning-rod effect), and the excitation of localized surface-plasmon resonances. Since the object of the experiments reported here is to compare the measured SH response from a metal surface with the results of jellium model calculations for a flat surface, it is important to consider the topography of the Al surfaces used in these experiments.

The morphology of atomically clean single-crystal surfaces at high temperatures is determined by thermodynamic considerations.[35] The surface evolves towards a configuration which minimizes the surface free energy. For high index planes which are not at a free-energy minimum, the surface may be unstable and facet to form a mixture of nearby low free-energy planes.[36] However, in the case of low-index surfaces which are at a free-energy minimum relative to neighboring surface planes, superatomic roughness must tend to smooth out with time. A simple diffusion model calculation[37] predicts that a hemispherical asperity of radius 1 μm, on an Al surface at a temperature of 450 °C, should flatten out in approximately 10 sec. Therefore, we do not expect any superatomic roughness to exist on our specimens after annealing has been completed. This conclusion is supported by the small spot diameters in the LEED diffraction patterns obtained from these specimens. From these widths, it is estimated that the typical domain size is approximately 100 Å.[38,39] Assuming the residual steps are monatomic, the surface height is modulated by tens of angstroms only over distances larger than 1000 Å.

The presence of monatomic steps on vicinal Si (Ref. 18) and Al (Ref. 19) surfaces has also been shown to produce enhancements of the measured SH signal. The results of Janz *et al.*[19] indicate that even at relatively low step densities as found on our Al surfaces, there may still be a measurable step contribution to the SH signal. However, as discussed in Sec. IV, this contribution may be identified by an anomalous dependence on temperature and oxygen exposure, and does not contribute significantly to the isotropic component of the SH response.

The optical arrangement was designed to measure the SH response of the specimen surface relative to the SH response of a single-crystal quartz plate. The light source is a synchronously pumped dye laser capable of operating at wavelengths between 565 and 870 nm. This laser emits a train of 3-psec pulses at a repetition rate of 76 MHz, with an average power ranging between 200 and 500 mw, depending on the operating wavelength. The laser beam is split into two using a glass-beam splitter. The reflected beam is directed through the reference arm containing a 1-mm-thick quartz plate cut with the c axis parallel to the plane of the plate. The transmitted beam is directed to the UHV chamber where it is focused to a 40-μm spot on the specimen surface. The polarization of this incident beam is controlled using a Soleil-Babinet compensator. From an equilibrium heat-flow calculation,[40] it is estimated that the maximum temperature rise of the surface due to localized heating by the laser is less than 9 °C. The SH light generated at the sample surface exits the UHV chamber and passes through colored glass filters and a Pellin-Broca dispersion prism which separates the SH light from the incident laser light. The SH signal is then detected using a photon-counting photomultiplier tube in a conventional chopped photon-counting configuration. The SH intensity measurements were made by collecting photon counts over periods ranging from 1 to 20 sec. depending on the SH intensity. The signal was tested, using filters and by varying the incident beam intensity, to confirm that it consisted entirely of SH light generated at the specimen surface. The reference beam was focused into the quartz plate where the SH light was generated in transmission and directed back onto the main beam path using a removable mirror, after which the reference SH beam was filtered and detected as before. By inserting or removing this mirror, it is possible to quickly alternate between the SH signal from the quartz plate and the Al surface. In practice, the SH signal from the Al surface was measured as the wavelength of the incident light was scanned over the range of the laser dye. The same scan was then repeated to obtain the SH signal from the quartz plate. The SH data from the Al surface was then normalized relative to the reference data from the quartz plate.

The susceptibility $\chi^{(2)}_{111}(2\omega)$ of quartz was used to calculate the SH intensity generated by the quartz plate. This calculation has been described in detail by Jerphagnon and Kurtz.[26] By multiplying the normalized SH data from the Al surfaces by the calculated intensity generated in the quartz plate, the value of R was obtained. Using this procedure, determinations of R were reproducible to within approximately $\pm 10\%$.

Experiments were also performed to measure the effect of oxygen exposure and temperature on the SH response. In the oxygen-exposure experiments, the SH intensity was monitored as the UHV chamber was filled with oxygen at a constant pressure of approximately 10^{-7} Torr. The temperature-dependence experiments were carried out by monitoring the SH intensity as the temperature was scanned between room temperature and 550 °C at a rate of 30 °C per minute.

IV. RESULTS AND DISCUSSION

In this section we describe the results of measurements of the magnitude, wavelength dependence, and anisotropy of the SH response of Al(111), Al(110), and Al(100) surfaces. Figure 2 shows the variation of the p-polarized SH intensity with rotation about the surface normal for an Al(111) surface, for a p-polarized incident beam at $\lambda = 630$, 730, and 820 nm. The measured SH intensity

displays an anisotropic dependence on rotation angle ψ of the form predicted by Eq. (8). From this dependence, the phase of A relative to B was determined to be zero within experimental error. Figure 3 shows the variation with wavelength of the measured SH reflectivities for the p-polarized light generated by a p-polarized incident beam at 67.5°, 45°, and 22.5° incidence on an Al(111) surface. For each angle of incidence two sets of data are shown, one taken for azimuthal angle $\psi=0°$, where the SH relectivity is given by $R=|A+B|^2$ [cf. Eq. (8)], and the other for $\psi=60°$, where $R=|A-B|^2$. The SH data exhibits an anisotropy which is small for $\lambda<600$ nm, but increases as λ increases out to 870 nm. However, the apparent increase in the anisotropy of the response with wavelength is largely due to a decrease in the magnitude of the isotropic SH response. When the data is inverted to obtain the anisotropic SH response parameter B in Eq. (8), we have found that $|B|$ increased by only 30% between $\lambda=630$ and 820 nm.

In order to determine whether the anisotropy is due to the intrinsic electronic structure of an ideally terminated surface, or due to surface morphology, the effect of oxygen exposure on the anisotropy of the SH signal was measured. The variation of the SH intensity with oxygen exposure for the SH maximum at $\psi=60°$ and for the SH minimum at $\psi=0°$ are shown in Fig. 4, for $\lambda=820$ nm. Typically, adsorption of oxygen onto a metal surface causes the SH signal to decrease monotonically until a saturation value is reached at approximately monolayer coverage.[7,8] This effect is thought to arise because the SH response of the surface electrons is much less when they are strongly bound in metal-oxygen bonds than when they are free.[7] However, on the Al(111) surface the anisotropic component of the SH signal disappears with an oxygen exposure of approximately 60 L, while the isotropic part of the SH signal reaches saturation only after 200 L [1 langmuir (L)$\equiv 10^{-6}$ Torr sec.]. When $\psi=0°$, the SH intensity increases upon initial oxygen exposure and then reverses direction and decays, though more slowly than the $\psi=60°$ signal, until the intensities at $\psi=0°$ and 60° are equal. Thereafter the SH signal decays at the same rate for both azimuthal positions. SH intensity was also checked at $\psi=30°$ for oxygen exposures between 0 and 200 L. The results of these measurements confirm that the SH response has become isotropic after approximately 60-L exposure. Therefore the magnitude of the anisotropic parameter B in Eq. (8) decreases with oxygen exposure three times more quickly than the isotropic response coefficient A.

The dependence on temperature of the SH signal from the (111) surface was also measured. In Fig. 5 we show the variation of the SH intensity at $\psi=0°$ and 60° as the temperature is raised at 30 °C per minute from room temperature to 500 °C. The temperature dependences of the

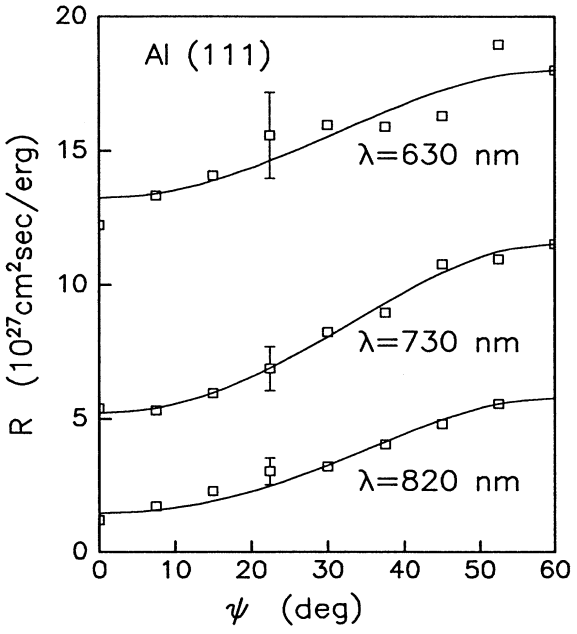

FIG. 2. The variation of the SH reflectivity R with azimuthal rotation ψ of the specimen about the surface normal for an Al(111) surface. The incident light and detected SH light are p polarized and the angle of incidence is 67.5°. The solid curve represents the best fit of Eq. (8) to the data.

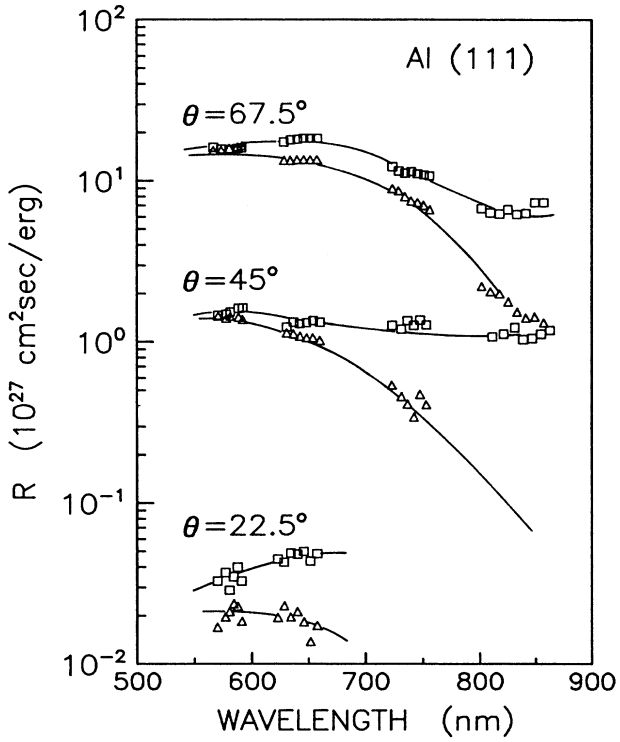

FIG. 3. The variation with incident wavelength of the p-polarized SH reflectivity R for an Al(111) surface with p-polarized light incident. Data are shown for angles of incidence of 67.5°, 45°, and 22.5°. The squares are the data for the maximum intensity at azimuthal position $\psi=60°$. The squares are the data for the maximum intensity at azimuthal position $\psi=60°$, and the triangles are the data for the minimum intensity at $\psi=0°$. The solid curves are meant to serve as a guide to the eye.

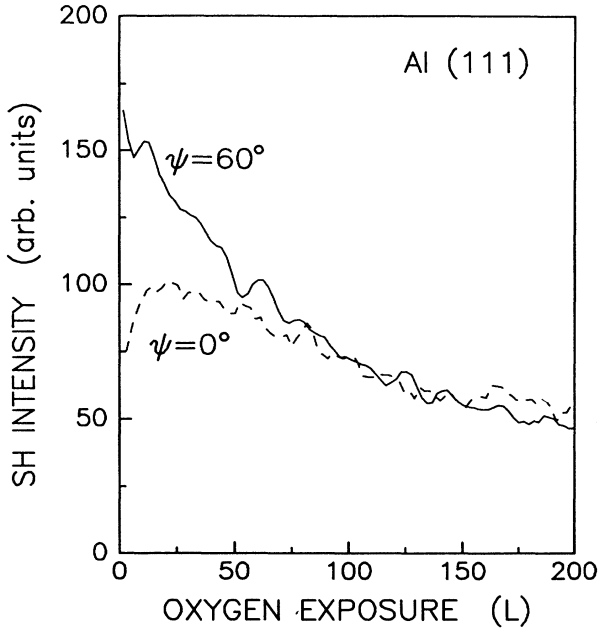

FIG. 4. The variation of the SH intensity with oxygen exposure for an Al(111) surface at the minimum ($\psi=0°$) and the maximum ($\psi=60°$) intensity azimuthal positions. The incident and detected SH light are p polarized, the angle of incidence is 67.5°, and $\lambda=820$ nm.

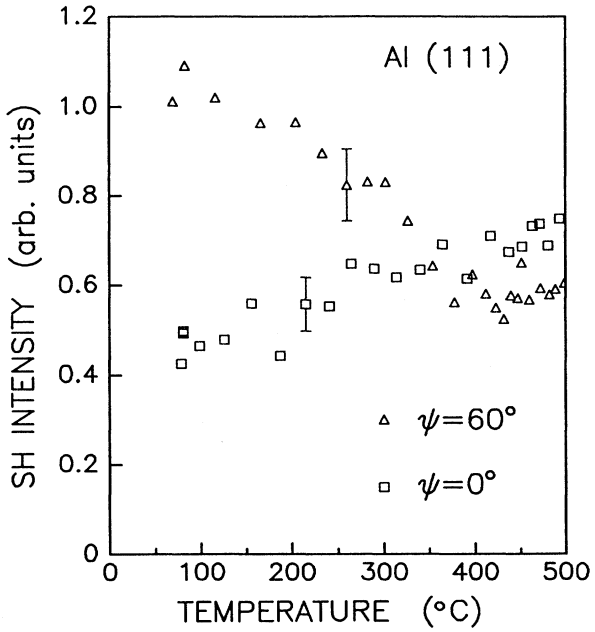

FIG. 5. The variation of the SH intensity with temperature for an Al(111) surface at the minimum ($\psi=0°$) and the maximum ($\psi=60°$) intensity azimuthal positions. The incident and detected SH light are p polarized, the angle of incidence is 67.5°, and $\lambda=820$ nm.

SH signal in the two azimuthal positions suggest that the anisotropic components of the SH signal decreases to zero as the temperature increases from 20 °C to 400 °C. At 450 °C, there was no detectable variation of the SH signal with azimuthal angle ψ, confirming that the anisotropic component of the SH response had vanished. The temperature dependence of the anisotropy is reversible upon cooling at a rate of approximately 20 °C per minute.

Anisotropy was also observed in the SH response from an Al(110) surface. The anisotropic response of the SH from this surface was found to have qualitatively the same dependence on λ, oxygen exposure, and temperature as the anisotropic part of the response of the Al(111) surface.

The anomalous behavior of the SH anisotropy upon heating the specimen or exposing it to oxygen is difficult to reconcile with the interpretation that the anisotropy is due to the electronic structure of an ideally terminated surface. Both the isotropic and anisotropic component of the SH response decay to an asymptotic value in less than 200-L oxygen exposure.[11] This exposure corresponds to the formation of a monolayer of oxygen on the Al surface.[41] Therefore both the isotropic and anisotropic parts of the SH response arise in the top one or two atomic layers of the Al surface, since a monolayer of surface oxygen will have little effect on deeper Al atoms. It has been demonstrated using medium-energy ion scattering (MEIS) that the (111) surface of Al remains well ordered at temperatures up to 0.5° below the bulk-melting temperature of 660 °C.[42] Therefore, raising the temperature from room temperature to 400 °C should not have a significant effect on the surface electronic structure. Furthermore, the fact that the anisotropy behaves the same on the Al(111) and the Al(110) surfaces suggests that the anisotropic response is not due to surface states because these will have different properties on different faces. Instead we require an anisotropic SH source which is common to both these surface orientations.

In previous work carried out in this laboratory, it has been demonstrated that the SH response of a stepped Al(100) surface can be significantly enhanced over that of a flat Al surface.[19] Relative to the flat surface signal, the step SH response varies strongly with wavelength and incident angle, growing monotonically with increasing wavelength and decreasing angle of incidence. The SH response from a stepped surface depends strongly on the relative orientation of the incident field and the step direction. It has also been shown that, due to preferential adsorption of oxygen at step edges,[19,43] the SH signal from the surface steps decays approximately three times faster with oxygen exposure than the signal from a flat surface. In subsequent work,[20] the enhanced SH signal from a stepped surface was found to decrease linearly with temperature as the temperature is raised from −100 °C to 500 °C. The step structure on surfaces of metals such as Cu (Ref. 44) and Ni (Refs. 45 and 46) is known to undergo roughening due to kink and defect formation even well below room temperature. This phenomenon may be related to the strong variation with temperature of the SH signal from a stepped metal surface. We note that such temperature dependence of the optical properties of stepped Al surfaces has been ob-

served in the photoemission experiments of Endriz and Spicer.[47] In these experiments, the surface-plasmon-assisted photoemission from a stepped surface decreased with increasing temperature, and returned reversibly to its initial level upon cooling. This result suggests that the changes in step structure with increasing temperature decreases the surface-plasmon photoemission from a stepped surface, as well as the SH susceptibility. The anisotropic SH response of a stepped vicinal Al(100) surface shows the same dependence on incident angle, oxygen exposure, temperature, and wavelength as the anisotropic part of the SH signal from the Al(111) and Al(110) surfaces reported here. The close parallels in the properties of the anisotropic SH response observed on the Al(111) and Al(110) surfaces and from stepped Al(100) surfaces suggests that they arise from the same source. We conclude that the anisotropic component of the SH response is probably due to the residual steps and surface topography remaining after specimen preparation. The orientation of surface steps on a surface will reflect the symmetry of the underlying lattice, so that the resulting anisotropic SH signal will still have the same symmetry as the crystal surface. As long as the dimension of the topographical features is much less than the wavelength of light, the phenomenological formalism of Sipe, Moss, and van Driel[13] for treating the anisotropic SH response of a surface remains applicable.

In this paper, we are primarily interested in the role of electronic structure in determining the SH response for the case of an ideally terminated single-crystal surface. Hence the isotropic component of the SH signal from the Al specimens was extracted from the data. This component, corresponding to the $|A|^2$ term in Eq. (8), does not exhibit any significant variation with temperature. Furthermore, the decay with oxygen exposure of the isotropic SH signal from the Al(111), Al(110), and Al(100) surfaces is consistent with the known sticking probabilities for oxygen adsorption on the respective surfaces. Therefore, the isotropic part of the SH signal (which could contain a contribution from the steps) is predominantly due to the intrinsic response of the low-index surface planes.

The dispersion characteristics of the isotropic component of the SH reflectivities are shown in Figs. 6, 7, and 8 for the Al(111), Al(110) and Al(100) surfaces, respectively. The SH reflectivity as a function of wavelength is shown for $\theta=67.5°$, 45°, and 22.5°. For all $\theta=22.5°$ and all surfaces the signal-to-noise restrictions limited data acquistion. Each data set in Fig. 6 is accompanied by an error bar indicating the estimated experimental uncertainty in R relative to data sets at other wavelength ranges and angles of incidence. Due to uncertainties in the reflectance and transmission of the optical components in the sample and reference arms of the experiment, there is also an uncertainty of approximately ±10% in the over all magnitude of the measured R. Also

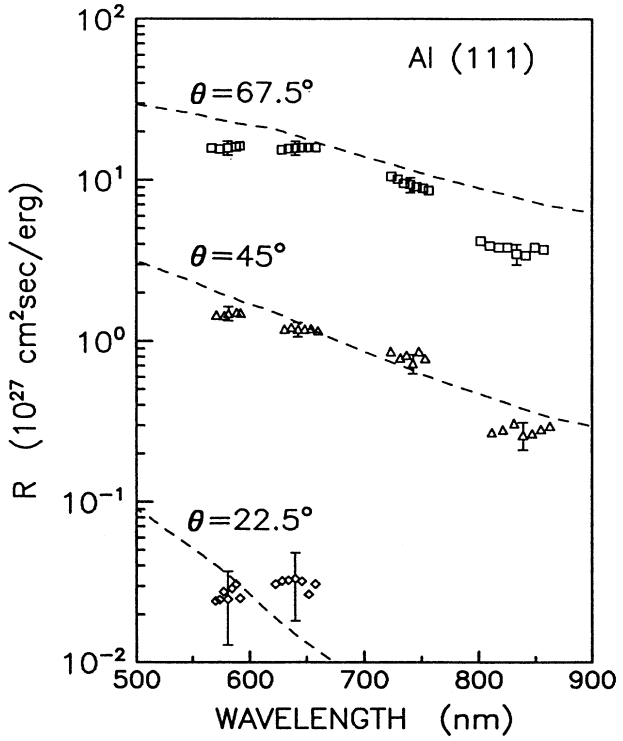

FIG. 6. The variation of the isotropic component of the SH reflectivity R with incident wavelength for an Al(111) surface at incident angles of 67.5° (squares), 45° (triangles), and 22.5° (diamonds). The incident and detected SH light are p polarized. The dashed lines represent the theoretical SH reflectivity obtained from the LDA-RPA results of Liebsch and Schaich (Ref. 4).

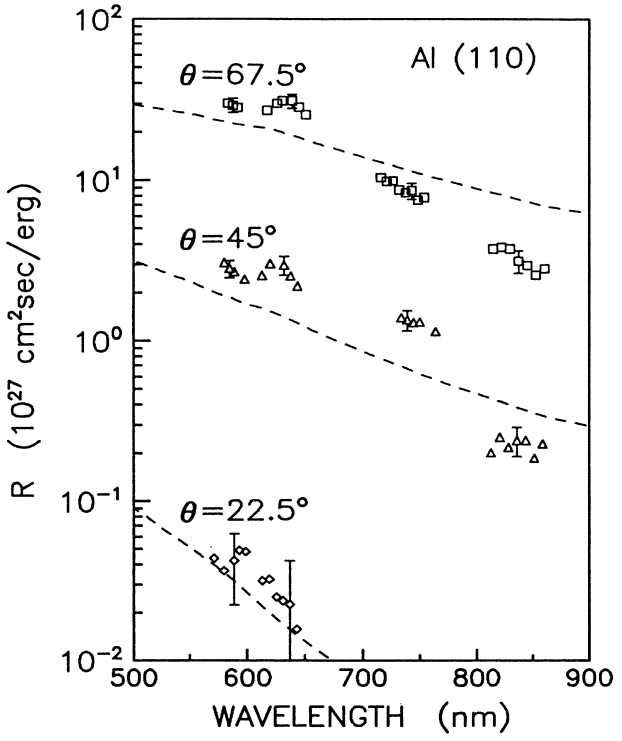

FIG. 7. Same as Fig. 6 except data are for an Al(110) surface.

shown in each graph is the theoretical SH reflectivity obtained from Eq. (7) using $a(\omega)$ obtained by Liebsch and Schaich[16] for the LDA-RPA calculation (see theory section). We have found that if the values for $a(\omega)$ calculated using the full TDLDA approach were used, the predictions for R were at least two times larger than our experimental results. In evaluating R from Eq. (7) and the calculated $a(\omega)$ coefficients, we used the dielectric function $\epsilon(\omega)$ of a free-electron metal with the same electron density as Al, rather than the dielectric function of real Al. As discussed in the theory section, the SH response coefficient $a(\omega)$ depends on the behavior of the linear fields in the surface region as well as the SH response of the electrons to those fields. Since $a(\omega)$ has been calculated using a jellium model, using a non-jellium model dielectric function to evaluate R would entail the convolution of two inequivalent models. The real dielectric function for Al is in fact well approximated by the free electron $\epsilon(\omega)$, despite the presence of the parallel band transitions at 1.5 eV ($\lambda \sim 800$ nm), so this approximation should not alter the theoretical prediction for R significantly.

The experimental and theoretical curves for the Al(111) surface show a similar dependence on wavelength, although the magnitude of the experimental R decreases more rapidly with increasing wavelength than the theoretical R. As a result the theoretical prediction for R at wavelengths longer than 800 nm is a factor of 2 larger than experiment. However, at shorter wavelengths the difference between experiment and theory decreases to within 20% for the R values at $\theta = 67.5°$ and 45°. The angle of incidence dependence of the SH signal also agrees well with the LDA-RPA theory, although this merely indicates that the SH polarization is dominated by the component oscillating normal to the surface [i.e., the $a(\omega)$ response]. Since R varies as $|a(\omega)|^2$, an agreement between experimental and theoretical R values within a factor of 2, as observed here, indicates that the calculated $a(\omega)$ is accurate to within 40%. Taking into consideration that we are comparing the SH response of a real metal surface with a jellium model calculation, the agreement is excellent.

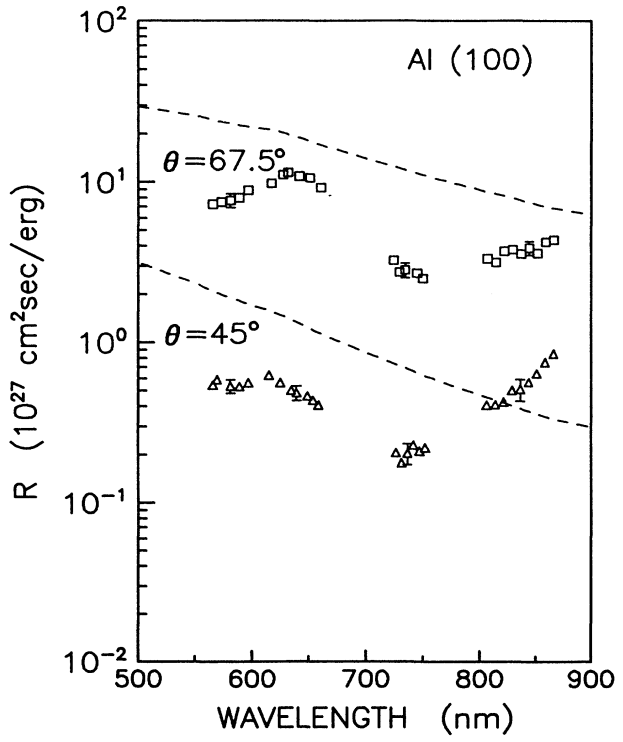

FIG. 8. Same as Fig. 6 except data are for an Al(100) surface.

Towards the short-wavelength end of the dispersion curves the experimental R levels off relative to the LDA-RPA calculation for all three surfaces. This is not understood at the present time. However, the SH photon energy for 600 nm (~ 2.1 eV) is near resonance with the work-function energy Φ (~ 4.2 eV) for the Al surface. The calculated $a(\omega)$ of Liebsch and Schaich exhibits resonant behavior, when the SH photon energy is near Φ, due to enhanced electron-hole pair creation at the surface. For the jellium model, this resonance is just discernable at $\lambda \sim 620$ nm in the calculated R calculated R curve shown in Figs. 6, 7, and 8. The electron-hole pair creation at the real Al surface may therefore also be affecting the SH response but to a much larger extent than for a jellium metal.

The wavelength dependence of R for the Al(110) surface is similar to that obtained from the (111) surface. The magnitude of R agrees with the jellium model predictions to within a factor of 2, and the SH data tend to decrease more rapidly with increasing wavelength than theory predicts. At wavelengths around 600 nm, R for an Al(110) surface is almost a factor of 2 larger than for the Al(111) surface, although the signal deceases more rapidly with wavelength so that the Al(110) and Al(100) results are the same at wavelengths longer than 800 nm.

The R values obtained for the Al(100) surface differ from the results obtained for the other two faces. The SH reflectivity is up to a factor of 3 smaller than the jellium model prediction for $\lambda < 800$ nm. Murphy *et al.*,[5] working at $\lambda = 1.06$ μm, have reported that the Al(100) surface gives a SH signal three times smaller than that obtained from the Al(111) surface. As suggested by Murphy *et al.* the decreased R probably occurs because the lattice potential has a stronger effect on the electrons on the (100) surface than on the (111) and (110) surfaces. The close agreement between the Al(111) and Al(110) results is consistent with work-function measurements for the three low-index surfaces of Al,[48] which show that the work-function energies Φ for the (111) and (110) surfaces are almost equal at 4.24 and 4.28 eV, respectively, while $\Phi = 4.41$ eV for the (100) face. These work-function results confirm that the electrons at the (100) surface are in fact more strongly bound than the electrons at the (111) and (110) surfaces, as suggested by the SH results. In bulk Al, the [200] Fourier component of the lattice pseudopotential the largest contribution to the total lattice potential.[49] If the influence of the pseudopotential extends to the surface region, then the ion contribution to the surface potential will be stronger at the (100) face than at

the other low-index surfaces. The strength of the lattice potential could be investigated by comparing self-consistent calculations of the screened potential for different low-index Al surfaces (e.g., see Ref. 50).

The frequency dependence of the SH signal from the (100) surface is also anomalous because R increases by a factor of 2 as λ increases from 750 to 860 nm at both 67.5° and 45° angles of incidence. The measurements of Murphy *et al.*[5] suggest that R has again fallen relative to the Al(111) signal at $\lambda=1.06$ μm, suggesting that there is a peak in R between 800 and 1000 nm. The SH photon energy in this wavelength range varies from 2.3 to 3.0 eV. The surface state at Γ on the Al(100) surface is located 2.75 eV below the Fermi energy.[51] Hence the rise in R at 800 nm may be attributed to a resonance of the SH photon energy and transitions from the surface state to empty bulk states just above the Fermi level. A similar surface-state resonance in the SH spectrum of Ag(110) has been reported by Urbach *et al.*[52] Unfortunately, since SH generation is surface specific, tests such as surface adsorption and disordering cannot unambiguously distinguish between the SH response due to a surface state and the response due to the vacuum tails of the bulk electron wave functions. Hence the assignment of this feature in the spectrum of Al(100) must await more complete measurements of the dispersion of R between $\lambda=750$ and 1000 nm.

The variation of the SH reflectivity with incident and SH light polarization was also measured for all three crystal surfaces. We found that there was no measurable component of s-polarized SH light at any wavelength or angle of incidence available to us. The p-polarized SH light was found to vary as $\cos^4\phi$ for all wavelengths and angles of incidence, as long as the plane of incidence was parallel to a symmetry plane of the surface. The result of a ϕ scan for Al(111) at $\lambda=580$ nm is shown as an example in Fig. 9. This result confirms that the isotropic SH polarization of the Al(111) surface is dominated by the normal surface polarization. The same result was obtained for the Al(110) and Al(100) surfaces. These results are consistent with the LDA-RPA and the full LDA calculations of Liebsch and Schaich,[16] which predict that $a(\omega)$ is much larger than $b(\omega)$ or $d(\omega)$.

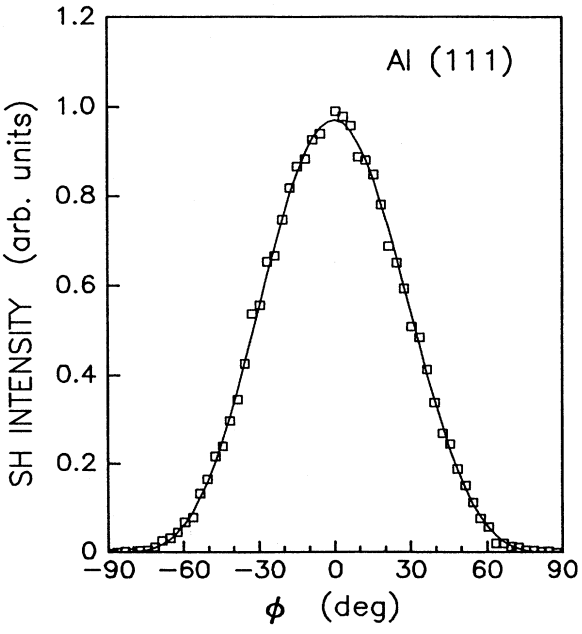

FIG. 9. The variation of the p-polarized SH intensity with incident light polarization angle ϕ for an Al(111) surface. The incident wavelength is 580 nm and the angle of incidence is 67.5°.

V. CONCLUSIONS

We have measured the SH reflectivity R of the Al(111), Al(110) and Al(100) surfaces between $\lambda=560$ and 860 nm. The SH response of the Al(111) and Al(110) surfaces is anisotropic, having the phenomenological form given in Eq. (8). The degree of anisotropy increases monotonically with increasing wavelength on both these surfaces. However, the anomalous dependence of the anisotropic component of the SH signal on temperature and on oxygen exposure suggests that the anisotropy is mainly due to microscopic topological features on the surface, such as steps, rather than intrinsic electronic structure. The isotropic component of R for the (111) and (110) surfaces agrees reasonably well in magnitude, polarization dependence, angle of incidence dependence, and wavelength dependence, with the theoretical R obtained for a jellium model calculated by Liebsch and Schaich[16] using the LDA-RPA method. This result confirms the suggestion by Liebsch and Schaich that the LDA approximation may not be accurate in the low-density tails of the electron wave functions at the surface, in which case the RPA response theory will give better results. On the other hand, we cannot exclude the possibility that the lattice potential at the (111) and (110) surfaces changes the response of the real surface compared with that of a jellium surface. If this is the case, then it is the jellium model itself which is inadequate rather than the LDA. The LDA calculation of the work function for Al in the jellium approximation[53] underestimates the work function of Al by 10%, suggesting that the jellium model may not provide a sufficiently accurate description of the Al surface to calculate the nonlinear response.

The SH response of the (100) surface differs from that of the other two crystal surfaces, as one might expect from the work-function measurements on these faces. R for Al(100) is approximately a factor of 3 smaller than the results for the (111) and (110) surfaces over wavelengths between 560 and 800 nm. This result is consistent with the measurements of Murphy *et al.* at 1.06 μm and indicates that the lattice potential has a much stronger effect on the (100) surface than on the (111) and (110) surfaces. Finally, the data for Al(100) at $\lambda>800$ nm suggests that there may be a resonant peak between 800 and 1000 nm due to the surface state at Γ on the (100) surface. However, more measurements of the dispersion of R throughout this wavelength range are necessary to confirm this.

In conclusion, our results indicate that the jellium cal-

culation of Liebsch and Schaich treats the surface electronic structure and the SH response accurately enough to give quantitative agreement with the isotropic response of a nearly-free-electron metal such as Al. Furthermore, we have found evidence that the anisotropic component of the SH response from the Al(111) and Al(110) surfaces arises from surface morphology rather than the intrinsic electronic structure of the Al surfaces. These results indicate that the jellium model is a reasonably accurate approximation for calculating the nonlinear response of the Al(111) and Al(110) surfaces. In the case of the Al(100) surface, on the other hand, both the suppression of the SH response relative to the Al(111) and Al(110) surface, and the possible presence of a surface-state resonance indicate that the effect of electronic band structure is more important. In order to obtain more insight into the role of the lattice potential on the electronic response, it would be interesting to adapt self-consistent LDA calculations to a model which incorporates a simple lattice pseudopotential.

ACKNOWLEDGMENTS

This work has been supported by the Natural Sciences and Engineering Research Council, the Ontario Laser and Lightwave Research Centre, and Alcan International Limited. We are grateful for the financial support to K. Pedersen from the Danish Natural Science and Engineering Research Council (Grant No. 11-7377). We would like to acknowledge the advice and assistance of R. Timsit in carrying out these experiments.

*Present address: University of Aalborg, Institute of Physics, Pontoppidanstrasse 103, 9220 Aalborg Øst, Denmark.

[1]Y. R. Shen, in *Chemistry and Structure at Interfaces: New Laser and Optical Techniques,* edited by R. B. Hall and A. B. Ellis (VCH, Deerfield Beach, FL, 1986), p. 151; G. L. Richmond, J. M. Robinson, and V. L. Shannon, Prog. Surf. Sci. **28**, 1 (1987).

[2]F. Brown, R. E. Parks, and A. M. Sleeper, Phys. Rev. Lett. **14**, 1029 (1965).

[3]F. Brown and R. E. Parks, Phys. Rev. Lett. **16**, 507 (1966).

[4]H. W. K. Tom and G. D. Aumiller, Phys. Rev. B **33**, 8818 (1986).

[5]R. Murphy, M. Yeganeh, K. J. Song, and E. W. Plummer, Phys. Rev. Lett. **63**, 318 (1989).

[6]J. M. Hicks, L. E. Urbach, E. W. Plummer, and H. L. Dai, Phys. Rev. Lett. **61**, 2588 (1988).

[7]H. W. K. Tom, C. M. Mate, X. D. Zhu, J. E. Crowell, T. F. Heinz, G. A. Somorjai, and Y. R. Shen, Phys. Rev. Lett. **52**, 348 (1984).

[8]R. J. M. Anderson and J. C. Hamilton, Phys. Rev. B **38**, 8451 (1988).

[9]T. F. Heinz, M. M. T. Loy, and W. A. Thompson, Phys. Rev. Lett. **54**, 63 (1985).

[10]G. L. Richmond, Surf. Sci. **147**, 116 (1984).

[11]S. Janz, K. Pedersen, R. S. Timsit, and H. M. van Driel, J. Vac. Sci. Tech. A (to be published).

[12]J. A. Litwin, J. E. Sipe, and H. M. van Driel, Phys. Rev. B **31**, 5543 (1983).

[13]J. E. Sipe, D. J. Moss, and H. M. van Driel, Phys. Rev. B **35**, 1129 (1987).

[14]J. Rudnick and E. A. Stern, Phys. Rev. B **4**, 4272 (1972).

[15]M. Corvi and W. L. Schaich, Phys. Rev. B **33**, 3688 (1986).

[16]A. Liebsch and W. L. Schaich, Phys. Rev. B **40**, 5401 (1989).

[17]A. Chizmeshya and E. Zaremba, Phys. Rev. B **37**, 2805 (1988).

[18]C. W. van Hasselt, M. A. Verheijen, and Th. Rasing, Phys. Rev. B **42**, 9263 (1990).

[19]S. Janz, D. J. Bottomley, R. S. Timsit, and H. M. van Driel, Phys. Rev. Lett. **66**, 1201 (1991).

[20]S. Janz, D. J. Bottomley, R. S. Timsit, and H. M. van Driel (unpublished).

[21]H. W. K. Tom, T. F. Heinz, and Y. R. Shen, Phys. Rev. Lett. **51**, 1983 (1983).

[22]S. A. Akhmanov, V. I. Emel'yanov, N. I. Koroteev, and V. N. Seminogov, Usp. Fiz. Nauk **147**, 675 (1985) [Sov. Phys.—Usp. **28**, 1084 (1985)].

[23]O. A. Aktsipetrov, I. M. Baranova, and Yu. A. Il'inskii, Zh. Eksp. Teor. Fiz. **91**, 287 (1986) [Sov. Phys.—JETP **64**, 167 (1986)].

[24]N. D. Lang and W. Kohn, Phys. Rev. B **1**, 4555 (1970).

[25]M. Weber and A. Liebsch, Phys. Rev. B **35**, 7411 (1987).

[26]J. Jerphagnon and S. K. Kurtz, J. Appl. Phys. **41**, 1667 (1970).

[27]*CRC Handbook of Laser Science and Technology,* edited by M. J. Weber (Commercial Rubber, Boca Raton, FL, 1986), Vol. 3, Pt. I, and references cited therein.

[28]R. C. Miller, Appl. Phys. Lett. **5**, 17 (1964).

[29]F. G. Parsons and R. K. Chang, Opt. Commun. **3**, 173 (1971).

[30]D. Bethune, A. J. Schmidt, and Y. R. Shen, Phys. Rev. B **11**, 3867 (1975).

[31]B. F. Levine, Phys. Rev. B **7**, 2600 (1973).

[32]C. K. Chen, T. F. Heinz, D. Ricard, and Y. R. Shen, Phys. Rev. B **27**, 1965 (1983).

[33]O. A. Aktsipetrov, A. A. Nikulin, V. I. Panov, S. I. Vasil'ev, and A. V. Petukhov, Solid State Commun. **76**, 55 (1990).

[34]G. T. Boyd, Th. Rasing, J. R. R. Leite, and Y. R. Shen, Phys. Rev. B **30**, 519 (1984).

[35]E. D. Williams and N. C. Bartelt, Science **251**, 393 (1991).

[36]D. W. Blakely and G. A. Somorjai, Surf. Sci. **65**, 419 (1977).

[37]R. S. Timsit, IEEE Trans. Compon. Hybrids Manufact. Technol. **CHMT-13**, 65 (1990).

[38]M. Henzler, Surf. Sci. **73**, 240 (1978).

[39]P. R. Pukite, C. S. Lent, and P. I. Cohen, Surf. Sci. **161**, 121 (1985).

[40]J. F. Ready, *Effects of High Power Laser Radiation* (Academic, New York, 1971), Chap. 3.

[41]C. W. B. Martinson and S. A. Flodström, Surf. Sci. **80**, 306 (1979).

[42]A. W. Denier van der Gon, R. J. Smith, J. M. Gay, D. J. O'Connor, and J. F. van der Veen, Surf. Sci. **227**, 143 (1990).

[43]A. L. Testoni and P. C. Stair, Surf. Sci. **171**, L149 (1986).

[44]M. den Nijs, E. K. Riedel, E. H. Conrad, and T. Engel, Phys. Rev. Lett. **55**, 1689 (1985).

[45]E. H. Conrad, R. M. Aten, D. S. Kaufman, L. R. Allen, T. Engel, M. den Nijs, and E. K. Riedel, J. Chem. Phys. **84**, 1015 (1986).

[46]K. S. Liang, E. B. Sirota, K. L. D,Amico, G. J. Hughes, and S. K. Sinha, Phys. Rev. Lett. **59**, 2447 (1987).

[47]J. G. Endriz and E. W. Spicer, Phys. Rev. B **4**, 4159 (1971).
[48]J. K. Grepstad, P. O. Gartland, and B. J. Slagsvold, Sur. Sci. **57**, 348 (1976).
[49]N. W. Ashcroft, Philos. Mag. **8**, 2055 (1963).
[50]D. Wang, A. J. Freeman, H. Krakauer, and M. Pasternak, Phys. Rev. B **23**, 1685 (1981).
[51]G. V. Hanson and S. A. Flodström, Phys. Rev. B **18**, 1562 (1978).
[52]L. E. Urbach, K. L. Percival, J. M. Hicks, E. W. Plummer, and H. L. Dai (unpublished).
[53]N. D. Lang and W. Kohn, Phys. Rev. B **3**, 1215 (1971).